Lipids in Health and Disease

RESEARCH

Open Access

Empagliflozin alleviates obesity-related cardiac dysfunction via the activation of SIRT3-mediated autophagosome formation

Youhong Luo[1†], Tongtong Ye[1†], Hongzhan Tian[1], Hongwei Song[1], Chengxia Kan[1], Fang Han[1,2], Ningning Hou[1], Xiaodong Sun[1*] and Jingwen Zhang[1*]

Abstract

Background Empagliflozin (EMPA) has demonstrated efficacy in providing cardiovascular benefits in metabolic diseases. However, the direct effect of EMPA on autophagy in obesity-related cardiac dysfunction remains unclear. Therefore, this study aimed to determine changes in cardiac autophagy during diet-induced obesity and clarify the exact mechanism by which EMPA regulates autophagic pathways.

Methods Male C57BL/6J mice were fed a 12-week high-fat diet (HFD) followed by 8 weeks of EMPA treatment. Body composition analysis and echocardiography were performed to evaluate metabolic alterations and cardiac function. Histological and immunofluorescence staining was used to evaluate potential enhancements in myocardial structure and biological function. Additionally, H9c2 cells were transfected with small interfering RNA targeting sirtuin 3 (SIRT3) and further treated with palmitic acid (PA) with or without EMPA. Autophagy-related targets were analyzed by western blotting and RT–qPCR.

Results EMPA administration effectively ameliorated metabolic disorders and cardiac diastolic dysfunction in HFD-fed mice. EMPA prevented obesity-induced myocardial hypertrophy, fibrosis, and inflammation through the activation of SIRT3-mediated autophagosome formation. The upregulation of SIRT3 triggered by EMPA promoted the initiation of autophagy by activating AMP-activated protein kinase (AMPK) and Beclin1. Furthermore, activated SIRT3 contributed to the elongation of autophagosomes through autophagy-related 4B cysteine peptidase (ATG4B) and autophagy-related 5 (ATG5).

Conclusions EMPA promotes SIRT3-mediated autophagosome formation to alleviate damage to the cardiac structure and function of obese mice. Activated SIRT3 initiates autophagy through AMPK/Beclin1 and further stimulates elongation of the autophagosome membrane via ATG4B/ATG5. These results provide a new explanation for the cardioprotective benefits of EMPA in obesity.

†Youhong Luo and Tongtong Ye contributed equally to this work and co-first author.

*Correspondence:
Xiaodong Sun
xiaodong.sun@sdsmu.edu.cn
Jingwen Zhang
fyjwzhang@sdsmu.edu.cn

Full list of author information is available at the end of the article

Keywords Obesity-related cardiac dysfunction, Empagliflozin, SIRT3, Autophagy

Background

Obesity is a significant public health concern because of its adverse effects on various organs [1]. Obesity-related cardiac dysfunction (ORCD) accounts for a large proportion of cardiovascular disease-related deaths worldwide. Obesity leads to increased myocardial hypertrophy and fibrosis, along with elevated levels of cardiac inflammation, resulting in adverse cardiac remodeling and dysfunction [2]. Therefore, a deeper understanding of the pathogenesis and molecular mechanisms is needed to promote effective therapeutic approaches for ORCD.

Sirtuin 3 (SIRT3), which is primarily found in mitochondria, is abundant in metabolically active tissues, such as the heart, kidney, brain, and liver. SIRT3 overexpression or activation can mitigate cardiac hypertrophy and fibrosis, suggesting its potential for cardiovascular disease therapy. The activation of SIRT3 through small ubiquitin-like modifier modifications has shown promise in reducing obesity and enhancing resistance to a high-fat diet (HFD) in mice [3]. However, obesity, particularly that induced by HFD feeding, leads to reduced SIRT3 expression, exacerbating cardiac dysfunction and remodeling. Therefore, strategies to increase myocardial SIRT3 activity or expression could offer novel therapeutic options for ORCD.

Autophagy acts as a cellular housekeeper to eliminate damaged proteins or cells under normal physiological and pathological conditions [4]. Numerous studies have shown that autophagy plays a crucial role in regulating various cell types, including atrial and ventricular myocytes, to maintain cardiac homeostasis [5, 6]. The activation of autophagy promotes cardiac protection against pressure overload-induced heart failure by preserving mitochondrial function [7]. However, excessive triglyceride accumulation in the hearts of individuals with obesity causes insulin resistance and diminished autophagy [8, 9], which are critical factors in the development of ORCD [10]. SIRT3 regulates autophagy through various pathways under diverse physiological conditions. SIRT3 triggers the AMP-activated protein kinase (AMPK)/Unc-51-like kinase 1 (ULK1) pathway to increase autophagy in adipocytes [11]. Moreover, SIRT3 promotes mitochondrial autophagy through PTEN-induced kinase 1 (PINK1)/Parkin to protect cardiac function in diabetic mice [12]. These findings further emphasize the central role of SIRT3 in promoting myocardial autophagy. Therefore, the identification of new drugs to stimulate SIRT3-mediated autophagy during obesity is necessary to address metabolic disorders in the heart.

Empagliflozin (EMPA), a representative sodium–glucose cotransporter 2 (SGLT2) inhibitor, promotes glucose excretion in urine, thereby reducing blood sugar concentrations by inhibiting its reabsorption in kidney tubules [13]. Clinical trials and meta-analyses have shown considerable cardiovascular protection in patients with diabetes treated with EMPA [14]. Notably, EMPA promotes renoprotective effects in diabetic mice by increasing autophagy. Furthermore, EMPA suppresses glycogen synthase kinase 3 beta (GSK3β) to inhibit excessive autophagy and protect against diabetic cardiomyopathy [15]. Nevertheless, the role of EMPA in regulating the level of autophagy in ORCD remains unclear. To address this knowledge gap, this study investigated the effects of EMPA intervention on obesity-induced myocardial histological damage and cardiac dysfunction in C57BL/6J mice fed a HFD for 12 weeks and further investigated alterations in autophagy-related signaling pathways. Moreover, the autophagy inhibitor 3-methyladenine (3-MA) was used in palmitic acid (PA)-treated H9c2 cells to address the effects of EMPA-mediated alterations in autophagy on lipid accumulation, cardiac cell hypertrophy, and inflammation. Finally, the role of SIRT3 in autophagy initiation and autophagosome elongation and formation mediated by EMPA was analyzed in PA-treated transfected H9c2 cells with/without EMPA.

Materials and methods

Experimental animals

Six-week-old male C57BL/6J mice (Pengyue, Jinan, China) were randomly separated into normal control (NC), HFD, and HFD plus EMPA (HFD-E) groups (8 mice/group). The mice in the HFD and HFD-E groups were fed a HFD (530 kcal/100 g, 60% fat, 20% protein, and 20% carbohydrate; Cat. #FB-D12492; Fanbo Biotechnology, Wuxi, China), whereas those in the NC group were fed a normal diet (320 kcal/100 g, 10% fat, 25% protein, and 65% carbohydrate; Fanbo Biotechnology, Wuxi, China). After 12 weeks, the mice in the HFD and HFD-E groups were subjected to vehicle or EMPA (10 mg/kg, diluted in saline with 0.5% hydroxyethylcellulose; Boehringer Ingelheim, Ingelheim, Germany) treatment by oral gavage once a day for 8 weeks. As a control, saline was administered to the NC group. Each mouse was maintained in a regular environment, and their fat/body weight ratio was determined via a Minispec LF50 device (Bruker, Hamburg, Germany). The Shandong Second Medical University Animal Ethics Committee approved the study protocol.

Measurement of glucose, triglyceride, and free fatty acid concentrations

The mice were subjected to glucose/insulin tolerance tests after receiving the above-described treatment for 20 weeks. After fasting for 6 h, the mice were either orally administered glucose (2 mg/g) or intraperitoneally injected with insulin (0.75 U/kg). The concentration of blood glucose at different time points was measured via a glucometer through the tail vein (Acon Biotech, Zhejiang, China). Following the establishment of the models, the mice were injected intraperitoneally with 2% sodium barbiturate (40 mg/kg). Serum was collected from blood samples. Kits (BC0625 and BC0596, Solarbio, Beijing, China) were used to measure the triglyceride (TG) and free fatty acid (FFA) concentrations in the serum.

Cell culture and treatments

H9c2 (2−1) cells were obtained from the Cell Bank of the Chinese Academy of Sciences (Shanghai, China). Dulbecco's modified Eagle's medium was used as the culture medium. The cell culture incubator provided a suitable environment at 37 °C with 5% CO_2. To establish a model of cellular lipotoxic injury, H9c2 cells were treated with PA. The experimental groups were divided into PA and PA with EMPA (PA-E) groups. In the control group, H9c2 cells were grown in normal DMEM. The cells in the PA group were stimulated with 500 μM PA (conjugated to BSA by the manufacturer) for 24 h, while the cells in the NC group were exposed to the solvent vehicle following the manufacturer's instructions (Cat. #KC004; Kunchuang Biotechnology, Xi'an, China). The cells in the PA+EMPA group were exposed to 500 μM PA and 1 μM EMPA (Boehringer Ingelheim, Ingelheim, Germany) for 24 h. EMPA was dissolved at a stock concentration of 1 mM in DMSO and subsequently diluted with culture medium (final concentration of 1 μM) with 0.1% DMSO. To study the role of autophagy in ORCD, H9c2 cells were pretreated with 10 mM 3-MA (Cat. #HY-19312; MedChemExpress, Shanghai, China) for 1 h before PA and EMPA treatment.

Echocardiographic evaluation

To assess cardiac function, the ejection fraction (EF), fractional shortening (FS), and early/late ventricular filling velocity (E/A) were detected via high-frequency ultrasound with a VINNO imaging system (Vinno Technology, Suzhou, China).

Histopathological analysis

The middle part of the left ventricular myocardial tissue from the mice was collected, fixed in 4% paraformaldehyde and sectioned into 5-μm-thick slices. Hematoxylin and eosin staining was used to evaluate the morphological structure, and Masson's trichrome staining was used to highlight the collagen fibers. Moreover, the middle part of the fresh left ventricular myocardial tissue was embedded in OCT gel and sectioned into 5-μm-thick slices via a freezing sectioning machine. Lipid accumulation in these sections was evaluated via Oil Red O staining. Micrographs were captured via a light microscope (Nikon, Tokyo, Japan). Subsequently, ImageJ software was used to analyze the Oil Red O staining and Masson's trichrome staining results of the myocardial tissue.

Immunofluorescence microscopy analysis of wheat germ agglutinin (WGA) and mitochondrial superoxide measurement

The fresh middle part of the left ventricular myocardial tissue from experimental mice was sectioned into 5-μm slices. The tissue slices were fixed in 4% paraformaldehyde and blocked with donkey serum after being permeabilized with 0.2% Triton X-100. The sections were then incubated with primary antibodies against LC3 (1:500; ab192890; Abcam, Cambridge, United Kingdom) and SIRT3 (1:500; 5490 S; Cell Signaling Technology, Danvers, USA) at 4 °C overnight. After secondary antibody incubation and DAPI staining, the samples were observed via a fluorescence microscope (Keyence, Shanghai, China). The cross-sectional area and mitochondrial superoxide production of myocytes were assessed by WGA agglutinin-Alexa Fluor 488 (W11261, Invitrogen, Thermo Fisher Scientific, Danvers, USA) and MitoSOX Red (M36008, Invitrogen, Thermo Fisher Scientific, Danvers, USA), respectively. In summary, 5-μm-thick fresh frozen mouse heart tissue sections were first rinsed in phosphate-buffered saline and then maintained at 37 °C with protection from light in phosphate-buffered saline buffer containing 5 μM MitoSOX Red and 10 μg/mL WGA. After blocking and washing, the slides were photographed via a fluorescence microscope (Keyence, Shanghai, China).

Western blotting

Total protein from tissue or H9c2 cells was electrophoresed on SDS–PAGE gels (20 μg/sample for cardiac tissue and 10 μg/sample for cellular proteins) and then transferred to a polyvinylidene difluoride membrane. The membranes were incubated with the primary antibody (1:1000) at 4 °C overnight, followed by incubation with the secondary antibody (1:5000) at room temperature for 1 h. The antibodies AMPK (5831 S), p-AMPK (2535 S, mTOR (2983 S), p-mTOR (5536 S), and SIRT3 (5490 S) were obtained from Cell Signaling Technology (Danvers, USA). The antibodies Beclin1 (ab207612, Abcam), ATG4B (ab154843, Abcam), and ATG5 (ab108327, Abcam) were obtained from Abcam (Cambridge, United Kingdom). The antibodies LC3 (NB100-2220, Novus Biologicals, Centennial, USA) and GAPDH (10494-1-AP, Proteintech, Wuhan, China) were also used as primary

antibodies. Immunoreactivity was detected via a Bio-Rad Laboratories imaging system (California, USA) to visualize the immunoreactive bands. The target proteins were normalized to GAPDH expression, and the final normalized density values were calculated.

Real-time quantitative PCR analysis

Total RNA was extracted from cardiac tissue via TRIzol reagent (Invitrogen, Thermo Fisher Scientific, Danvers, USA) from left ventricular myocardial tissue. The volume of RNA was adjusted according to the concentration (1000 ng/μL). TB Green® Premix Ex Taq™ II (#RR820A; TaKaRa, Shiga, Japan) was used to perform reverse transcription with purified cDNA obtained from the PrimeScript™ RT Reagent Kit (#RR047A; TaKaRa, Shiga, Japan). The final amplification was performed via certain primers (Appendix Table 1 in Additional file 1). *Gapdh* was used as a control, and values were calculated via the 2^-(ΔΔCt) method to determine its relative expression level.

Small interfering RNA transfection

The knockdown of SIRT3 was carried out with small interfering RNA (siSIRT3) produced by Heyuan Biotechnology (Cat. #RY200297; Shanghai, China; Appendix Table 2 in Additional file 1). The siSIRT3 or scrambled siRNA was transiently transfected into the cells. The cells were inoculated into 6-well plates at 150,000 cells/well and transfected at 50–60% confluency. Lipo3000 transfection reagent (Invitrogen, Thermo Fisher Scientific, Danvers, USA) was mixed with the siRNA according to the manufacturer's instructions to form a Lipo3000-RNA complex. The complex was added evenly to a Petri dish and incubated in an incubator for 72 h before proceeding to the next step.

Cell hypertrophy and lipid accumulation

H9c2 cardiomyocytes were divided into NC, PA, PA-E, and PA-E+3-MA groups. The morphology and Oil Red O staining (G1262, Solarbio, Beijing, China) of the cells in each group were observed and photographed under a microscope. The surface area of the cells and the positive area of Oil Red O staining were calculated via ImageJ software. Multiple observation fields were selected for each group, and at least 60 cardiomyocytes were randomly chosen for analysis.

Statistical analysis

The normally distributed data are presented as the mean±SEM. Statistical comparisons between two samples were performed via unpaired Student's t test, whereas comparisons between multiple samples were performed via one-way or two-way ANOVA with Tukey's post hoc test. GraphPad Prism 8.3.0 software (California, USA) was used for the analyses, and statistical significance was set at $P<0.05$.

Results

EMPA prevents metabolic disorders in HFD-fed mice

After a 12-week HFD protocol, notable increases in body weight and fat mass were observed (Fig. 1A-E). However, compared with obese mice, treatment with EMPA for 8 weeks restrained further body weight/fat mass increases (Fig. 1A-E). Furthermore, compared with NC mice, HFD-fed mice presented decreased insulin and glucose tolerance, which was significantly improved by EMPA treatment (Fig. 1F and G). To further assess lipid metabolism in the mice, the serum TG and FFA levels were measured. Compared with those in the NC group, the TG and FFA levels in the HFD group were greater. EMPA treatment significantly reduced TG levels but not FFA levels (Fig. 1H and I).

EMPA mitigates obesity-induced cardiac histological damage and myocardial inflammation

After the experiments, cardiac ultrasonography was performed to evaluate how EMPA affects heart function. The results revealed that systolic function, as shown by the EF and FS, did not significantly differ between the groups (Fig. 2A). This finding indicated that HFD-induced obesity had a minimal effect on myocardial systolic function. The mitral flow E/A ratio was dramatically reduced in the HFD group and reversed by EMPA, indicating that EMPA could inhibit obesity-induced cardiac diastolic dysfunction (Fig. 2B). Histopathological analysis of myocardial tissues revealed disrupted and enlarged cardiomyocytes with increased fibrosis in HFD-fed hearts. However, the myocardial tissue structure was more orderly, and the fibrotic area and cardiomyocyte size were significantly reduced in HFD-fed hearts after EMPA administration (Fig. 2C). Oil Red O staining of cardiac sections from HFD-fed mice revealed a significant increase in the number of neutral lipid droplets compared with NC mice, whereas EMPA treatment significantly reduced the number of lipid droplets in HFD-fed mice (Fig. 2C). The MitoSOX Red fluorescent probe was used to measure the generation of superoxide within the mitochondria to evaluate the role of EMPA in controlling redox homeostasis in the heart. Superoxide production in the mitochondria of the HFD-fed group was significantly greater than that in the mitochondria of the NC group, and EMPA significantly reduced mitochondrial superoxide production (Fig. 2C). WGA staining revealed greater myocardial hypertrophy in HFD-fed hearts than in NC hearts, whereas EMPA significantly suppressed obesity-induced myocardial hypertrophy (Fig. 2C).

Fibrosis-related genes were further detected because EMPA effectively alleviated obesity-induced myocardial

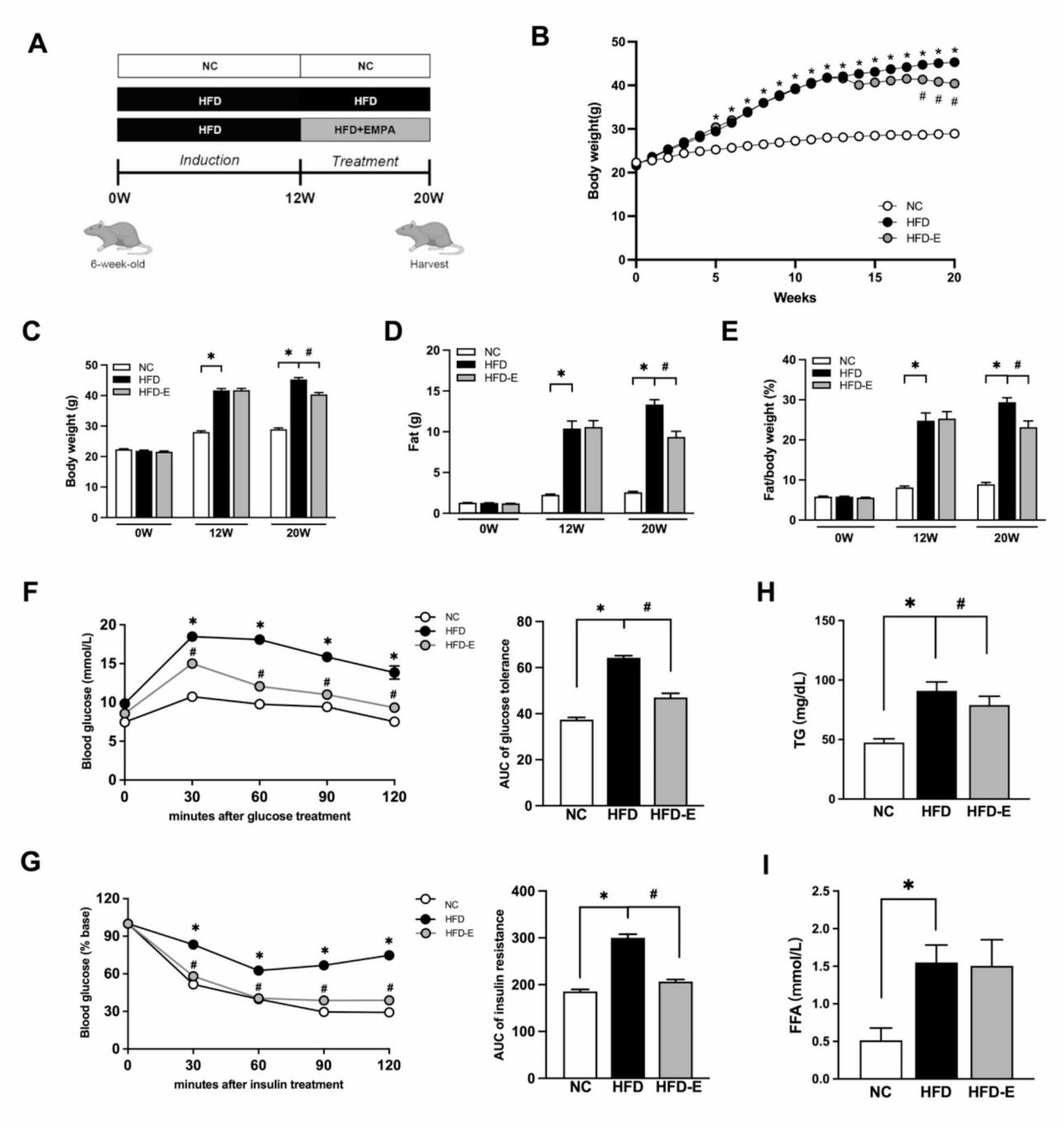

Fig. 1 Changes in metabolic profiles after the EMPA intervention in HFD-fed mice. (**A**) Treatment scheme for the control and obese animals. (**B**) The body weights of the NC, HFD, and HFD-E groups were measured each week. (**C**-**E**) Effects of EMPA on the body weight (**C**), body fat (**D**), and percentage of body fat/body weight (**E**) in obese mice. (**F**) Glucose tolerance. (**G**) Insulin tolerance. (**H**) Triglycerides. (**I**) Free fatty acids. $N = 4–6$ mice/group. $^{*}P < 0.05$ vs. NC; $^{\#}P < 0.05$ vs. HFD

histological damage. The mRNA levels of *Acta2*, *Tgfb1*, *Col1a1*, and *Nppb* appear to be responsible for the development of cardiac fibrosis and cardiac hypertrophy [16]. HFD-fed hearts presented increased mRNA levels of *Acta2*, *Tgfb1*, *Col1a1*, and *Nppb*, and EMPA suppressed this marked profibrotic cellular phenotype (Fig. 2D).

Additionally, the mRNA levels of inflammatory factors in cardiac tissue were assessed via qPCR. The obesity-induced chronic inflammatory response leads to a greatly increased risk of cardiovascular disease [17]. In HFD-fed hearts, the expression of inflammation-associated genes (*Nlrp3*, *Il-1b*, *Tnf*, and *Il-18*) was significantly greater

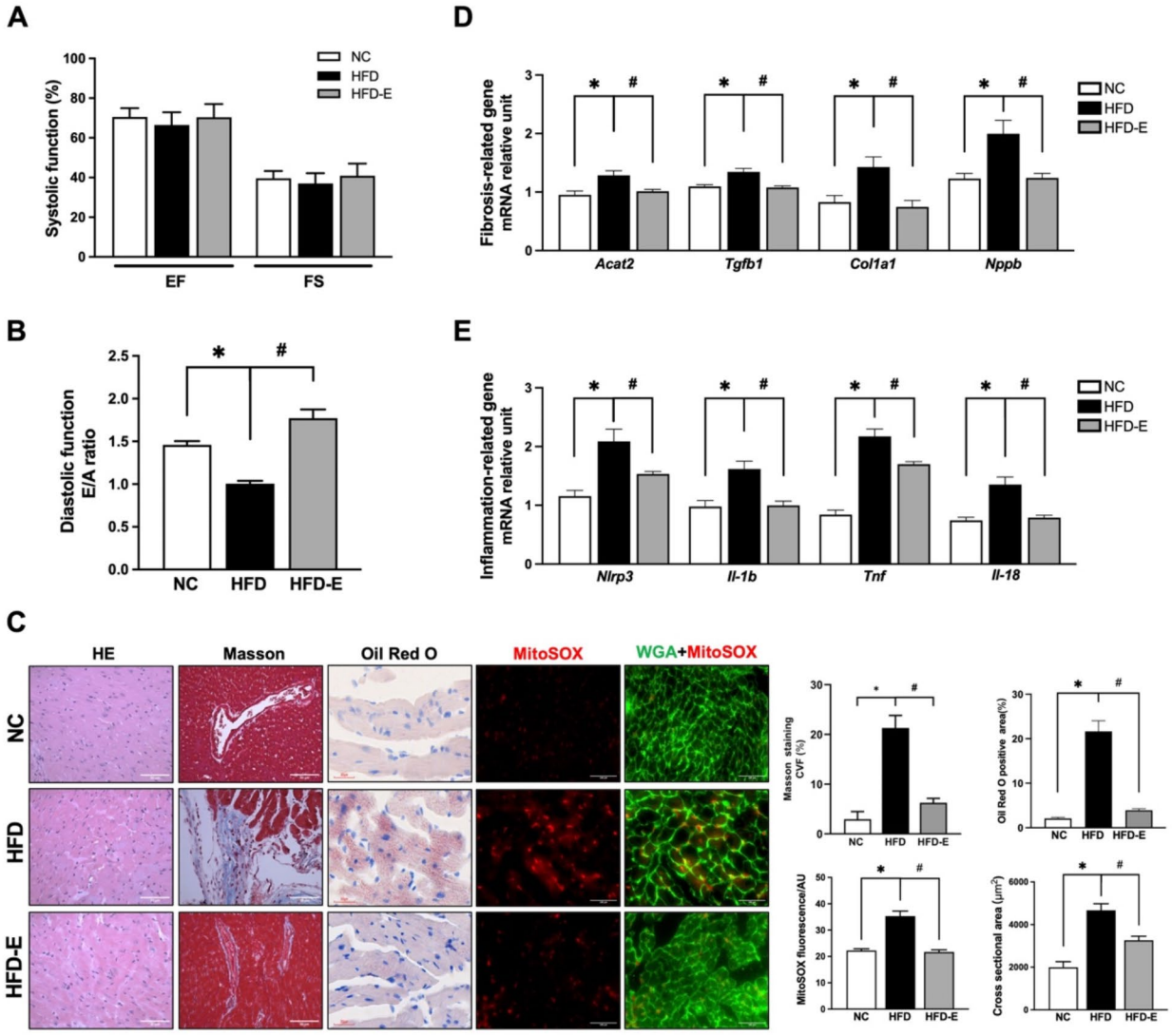

Fig. 2 Assessment of cardiac structure and function after EMPA treatment in HFD-fed mice. (**A**) Cardiac systolic function. (**B**) Cardiac diastolic function. (**C**) Histological alterations, fibrosis status, and lipid accumulation were evaluated in cardiac ventricle tissue. Scale bar = 30 μm. Mitochondrial superoxide levels and the myocardial cross-sectional area were detected via MitoSOX and WGA staining. Scale bar = 100 μm. (**D**) Myocardial fibrosis-related genes. (**E**) Myocardial inflammation-related genes (*Tnf*, *Nlrp3*, *IL-1β*, *and IL-18*). $N = 4–6$ mice/group. $^{*}P < 0.05$ vs. NC; $^{\#}P < 0.05$ vs. HFD

than that in NC hearts, while the expression of these inflammatory biomarkers was inhibited by EMPA administration (Fig. 2E). These results indicate that EMPA is a powerful approach to mitigate obesity-induced cardiac hypertrophy and myocardial inflammation.

EMPA upregulates cardiac SIRT3 and activates autophagosome formation

SIRT3, which is highly expressed in cardiac muscle, maintains the redox balance and regulates autophagy in the heart under various conditions [18, 19]. EMPA treatment increased the levels of the SIRT3 protein and *Sirt3* mRNA in the HFD-fed group (Fig. 3A and B). Autophagy is responsible for cardiac homeostasis, and its alterations accelerate the damage caused by cardiac hypertrophy and fibrosis [20]. A critical marker for autophagy is the formation of an autophagosome, which is an isolation membrane that surrounds cytoplasmic organelles and proteins, and LC3 II is an autophagosome marker [21]. Therefore, the levels of LC3 II in HFD-fed mice were evaluated to determine the effect of EMPA on this autophagosome marker. The results revealed that cardiac LC3 levels and the LC3 II/LC3 I ratio, as well as *Map1lc3b* mRNA levels (encoding for LC3), were increased after EMPA treatment (Fig. 3C and D).

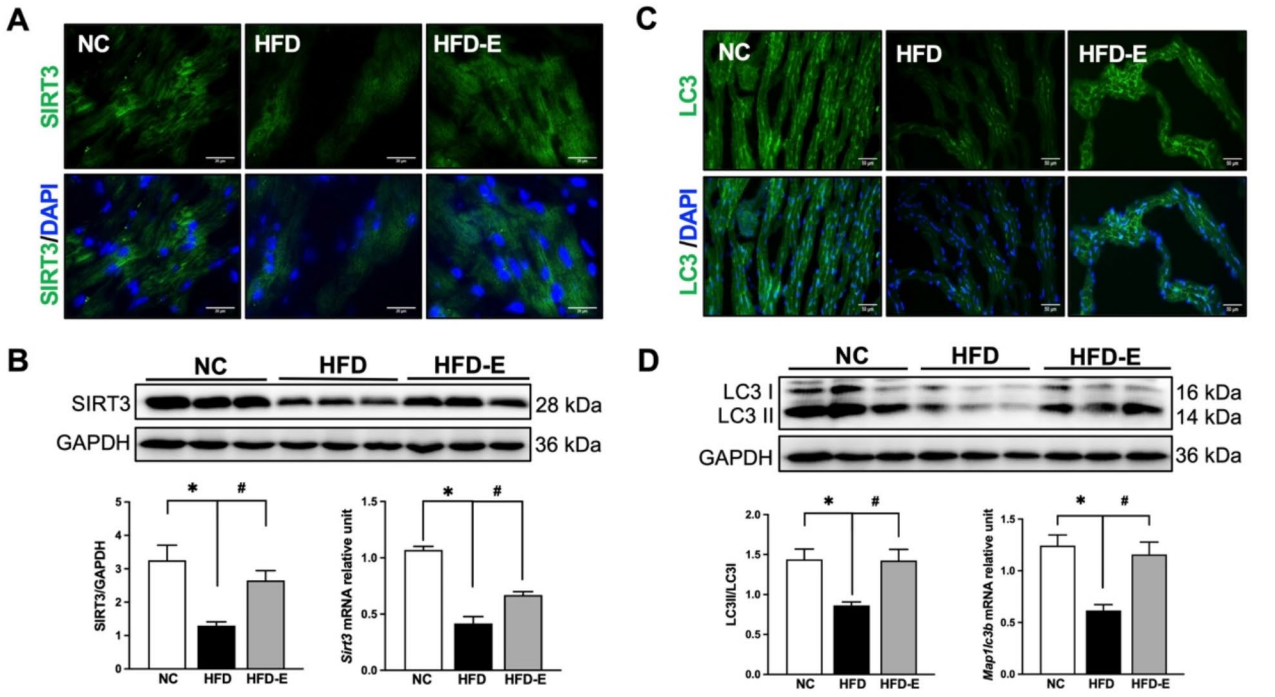

Fig. 3 EMPA upregulates cardiac SIRT3 and activates autophagosome formation. (**A**) Comparison of SIRT3 expression in the myocardium. Scale bar = 20 μm. (**B**) SIRT3 levels. (**C**) Evaluation of LC3 expression levels in myocardial tissues. Scale bar = 50 μm. (**D**) LC3 II/I protein levels and the mRNA levels of LC3 (*Map1lc3b*). $N = 4–6$ mice/group. $^{*}P < 0.05$ vs. NC; $^{\#}P < 0.05$ vs. HFD

EMPA facilitates the multiple steps of autophagosome formation

AMPK facilitates the initiation of autophagy by inhibiting mTOR activity [22]. In the hearts of HFD-fed mice, the phosphorylation of AMPK at Thr172 was reduced, whereas the hyperphosphorylation of mTOR was increased, suggesting that the initiation of autophagy was blocked in obese hearts. EMPA intervention triggered autophagy initiation in HFD-fed hearts by promoting the phosphorylation of AMPK and inhibiting mTOR phosphorylation (Fig. 4A). On the other hand, Beclin1 is another key regulatory protein of autophagy because it contributes to autophagosome membrane formation [23]. The protein level of Beclin1 was downregulated upon HFD feeding and significantly elevated after EMPA treatment (Fig. 4A). In addition, the autophagy-related (ATG) gene-mediated ATG5–ATG12–ATG16L1 complex and the processing of LC3 contribute to elongation of the phagophore [24]. The results revealed downregulated protein expression of ATG4B and ATG5 in the cardiac tissues of HFD-fed mice, but this expression was significantly increased following EMPA treatment (Fig. 4B). Moreover, the mRNA levels of *Becn1* and autophagy-promoting proteins (ATGs) in mouse heart tissues across treatments were detected. The results revealed significant reductions in the mRNA levels of *Becn1* and four ATGs (*Atg4b*, *Atg5*, *Atg9a*, *and Atg16l1*) in HFD-fed mice, whereas EMPA intervention elevated the mRNA levels of *Becn1* and four ATGs (*Atg4b*, *Atg5*, *Atg9a*, *and Atg16l1*) (Fig. 4C). These findings suggest that EMPA promotes multiple steps of autophagosome formation, including the initiation of autophagosome formation through AMPK-mTOR and Beclin1 and ATG4B/ATG5-induced elongation, which protects the heart from ORCD.

EMPA promotes the initiation of autophagy and autophagosome membrane elongation in cardiomyocytes via SIRT3 activation

A lipotoxicity model in H9c2 cells was induced with PA to verify the protective effect of EMPA against ORCD. The results revealed that the LC3 II/LC3 I protein levels were decreased after PA treatment, whereas the *Col1a1* and *Tnf* mRNA levels, cardiomyocyte area, and positive area of Oil Red O were increased (Fig. 5A-D). However, these effects were reversed by EMPA, which increased LC3 II/LC3 I protein levels, reduced *Col1a1* and *Tnf* mRNA levels, and decreased the cardiomyocyte area and positive area of Oil Red O (Fig. 5A-D). Treatment with 3-MA, which inhibits autophagy, abolished the protective effects of EMPA on cardiomyocytes (Fig. 5A-D), indicating the involvement of autophagy in EMPA-mediated protection against ORCD.

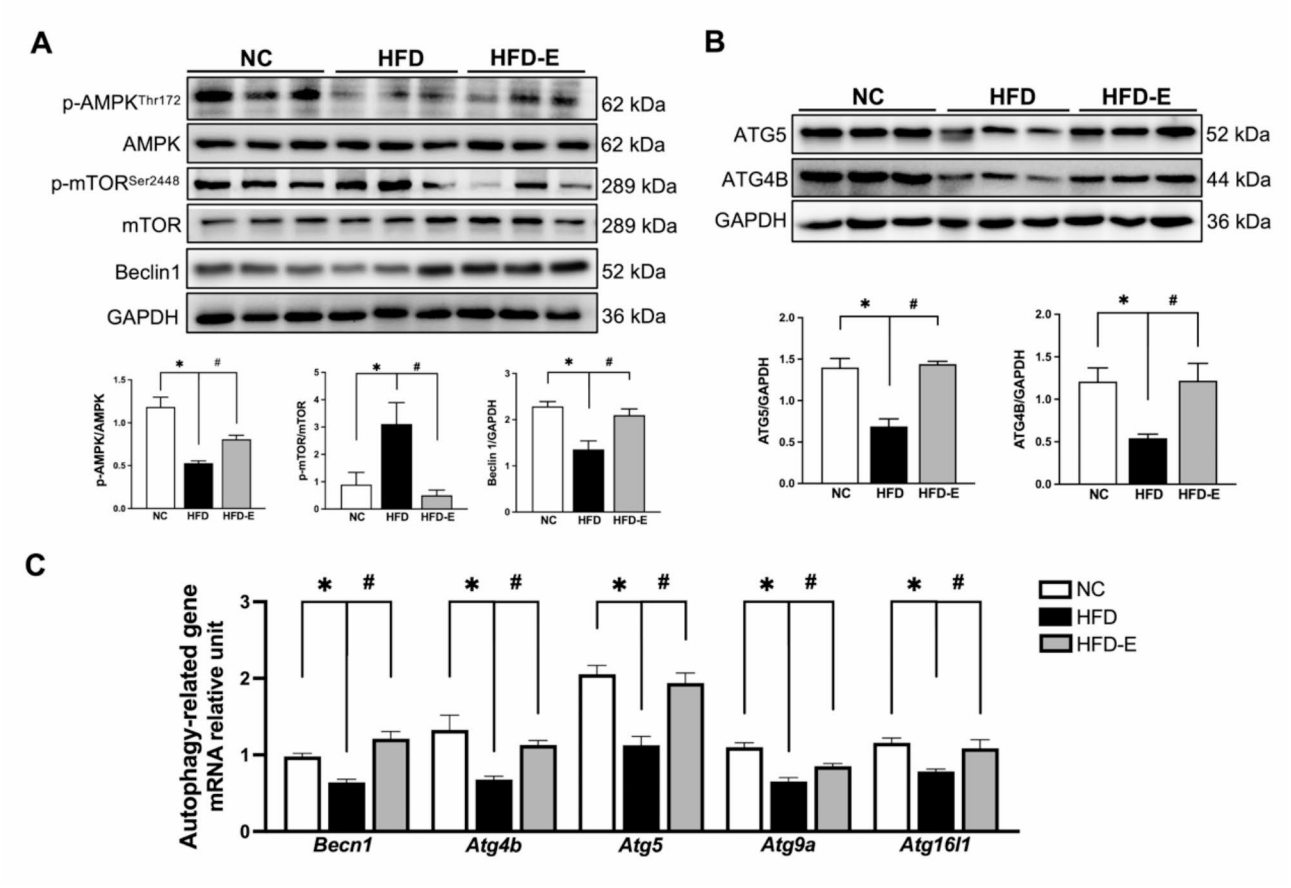

Fig. 4 EMPA facilitates multiple steps of autophagosome formation. (**A**) The levels of p-AMPK^{Thr172}, AMPK, p-mTOR^{Ser248}, mTOR and Beclin1. (**B**) The protein levels of ATG4B and ATG5. (**C**) Autophagy-related genes. $N = 4–6$ mice/group. $^{*}P < 0.05$ vs. NC; $^{\#}P < 0.05$ vs. HFD

Additionally, to address whether EMPA-promoted autophagosome formation in obese hearts is mediated by SIRT3, siRNA-transfected H9c2s were subjected to PA with or without EMPA treatment. After SIRT3 silencing, EMPA did not reverse the reduction in the LC3 II/LC3 I ratio (Fig. 6A–C), suggesting that EMPA alleviates ORCD through the activation of SIRT3. Furthermore, EMPA did not promote the phosphorylation of AMPK or the phosphorylation of mTOR after PA treatment in SIRT3-knockdown H9c2 cells (Fig. 6D–F). EMPA also failed to upregulate Beclin1 in PA-treated SIRT3-knockdown cells (Fig. 6D and G). These findings suggest that EMPA promotes AMPK/mTOR- and Beclin1-mediated initiation of autophagy to alleviate ORCD by activating SIRT3. Moreover, EMPA-induced upregulation of ATG4B and ATG5 was not observed in SIRT3-knockdown cells during PA treatment (Fig. 6D, H, and I). These findings indicate that SIRT3 is a key cardiac target through which EMPA initiates the ATG4B/ATG5 cascade.

Discussion

Both clinical findings and experimental studies provide compelling evidence that the cardiorenal benefits of SGLT2 inhibitors are associated with the activation of nutrient deprivation signaling [25, 26]. Energy sensors (mTOR, AMPK, and sirtuin) play a role in the interplay between cellular stress and survival through the autophagic process [25, 26]. This study accurately revealed the importance of their intracellular actions, as EMPA attenuated obesity-induced myocardial hypertrophy, fibrosis, inflammation and cardiac dysfunction via SIRT3-mediated autophagic signaling pathways. EMPA promoted SIRT3 expression in the myocardium of obese mice, which further initiated autophagy via AMPK/Beclin1 and activated ATG4B/ATG5 to induce the elongation of autophagosome membranes (Fig. 7).

Obesity leads to cardiac remodeling in the form of ventricular hypertrophy and myocardial fibrosis [27], and it is an important exogenous factor involved in causing a systemic chronic inflammatory state [28]. Both of these processes ultimately lead to the development of cardiovascular disease, particularly heart failure [29]. With approval by the FDA, the SGLT2 inhibitor EMPA has

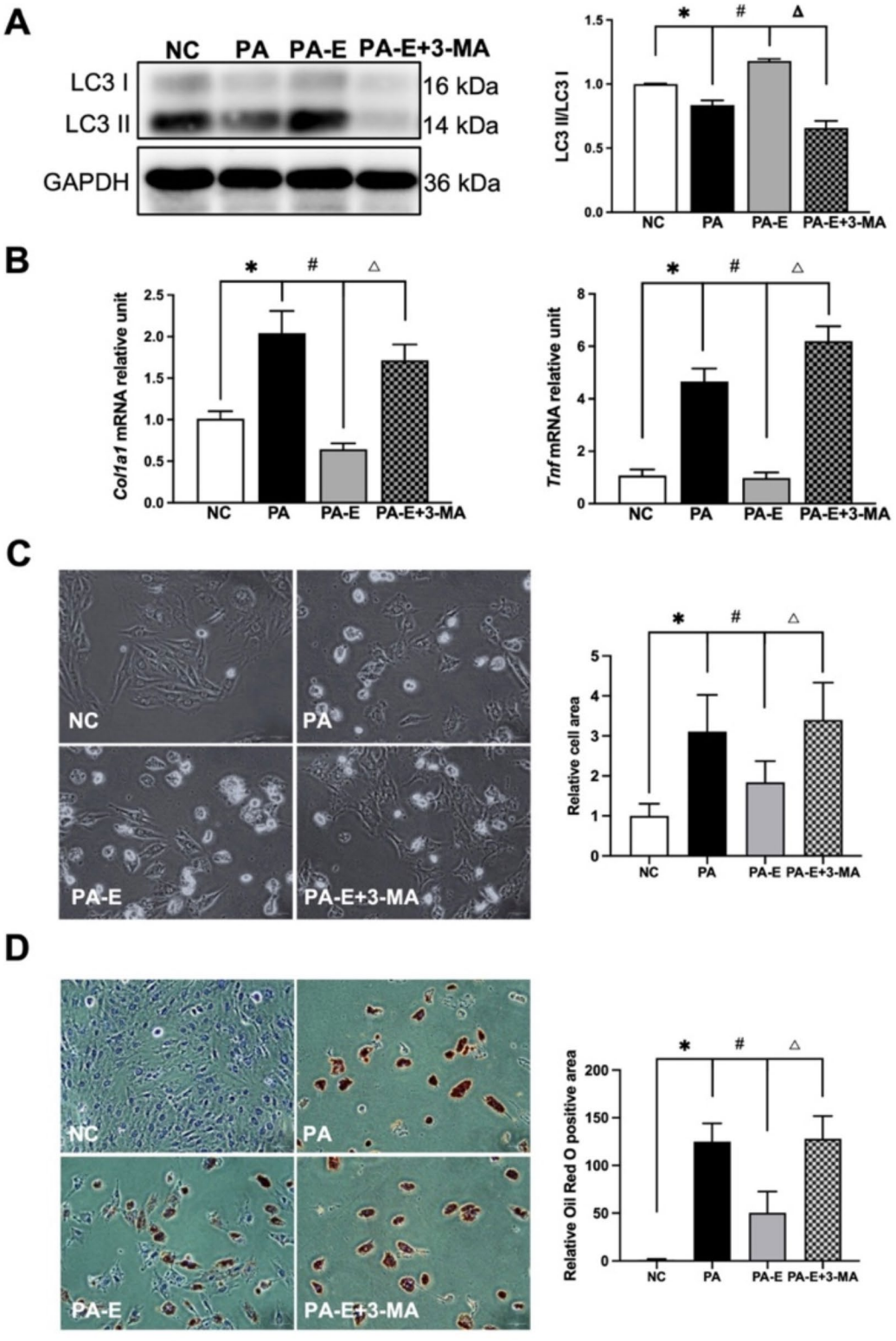

Fig. 5 EMPA promotes autophagosome formation to inhibit obesity-related myocardial inflammation, fibrosis, and hypertrophy. (**A**) LC3 II/LC3 I levels. (**B**) Alterations in myocardial fibrosis-related gene expression (*Col1a1*) and the level of an inflammatory cytokine (*Tnf*). (**C**) Impact on the area of H9c2 cells was measured. (**D**) Oil Red O-positive area in H9c2 cells. $N = 3$ biological replicates, and each replicate included > 60 cells. $^{*}P < 0.05$ vs. NC; $^{\#}P < 0.05$ vs. PA; $^{\Delta}P < 0.05$ vs. PA-E

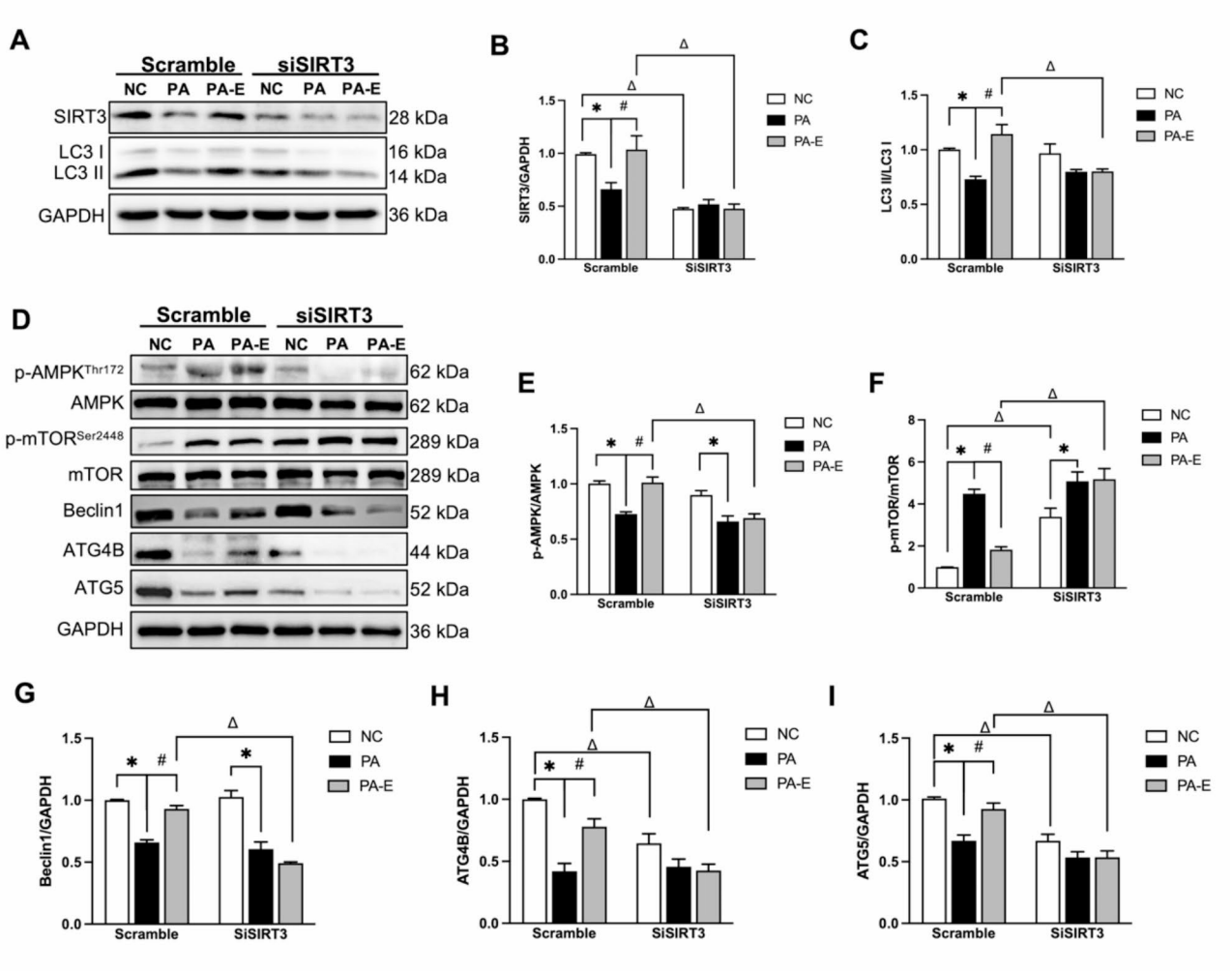

Fig. 6 EMPA promotes autophagy initiation and autophagosome membrane elongation in cardiomyocytes via SIRT3 activation. (**A**-**C**) H9c2 cells were transfected with siSIRT3 or scrambled siRNA and then subjected to 0.5 mM PA with or without 1 μM EMPA. The protein levels of SIRT3 and LC3 II/LC3 I were detected. (**D**-**I**) The protein levels of genes related to autophagy initiation (p-AMPK^{Thr172}, AMPK, p-mTOR^{Ser248}, mTOR, and Beclin1) and autophagosome elongation (ATG4B and ATG5) were detected in transfected cells. $N=3$ biological replicates. $^{*}P<0.05$ vs. NC; $^{\#}P<0.05$ vs. PA; $^{\Delta}P<0.05$ vs. Scramble

become an oral hypoglycemic agent for reducing cardiovascular risk [30, 31]. The unique pharmacological mechanism of action of EMPA has attracted widespread attention and research interest in the medical community. Several previous studies reported that EMPA improved ORCD [32]. Previous studies have also shown that EMPA improved insulin resistance by reducing glucose reabsorption to lower blood glucose concentrations in obese mice, which in turn reduced insulin demand in obese mice. In addition, EMPA can regulate blood lipids and reduce TG concentrations [33]. This study examined the protective effects of EMPA on the heart of obese mice and demonstrated its efficacy in improving myocardial hypertrophy and fibrosis, attenuating inflammation, and preserving normal cardiac structure and function.

Notably, the mechanism of action of EMPA is closely related to that of SIRT3, which is an important metabolic regulator. In this study, EMPA intervention upregulated SIRT3 expression in the myocardial tissue of obese mice. SIRT3 is crucial for cellular metabolism and has the potential to treat obesity and its complications. The involvement of SIRT3 in regulating energy metabolism, oxidative stress, and cellular autophagy through deacetylase activity is well established [34]. However, in obesity, SIRT3 function in cardiac tissue decreases, potentially rendering cardiomyocytes more susceptible to obesity-induced damage. Therefore, investigating the mechanism of action of SIRT3 in obese hearts is important for understanding the pathogenesis of ORCD.

Autophagy, a well-known degradation process, acts as an essential regulator to maintain cardiac homeostasis. Metformin enhances autophagy and provides cardioprotection in dilated cardiomyopathy [35]. Dysregulated autophagy is implicated in the onset of ORCD. It has

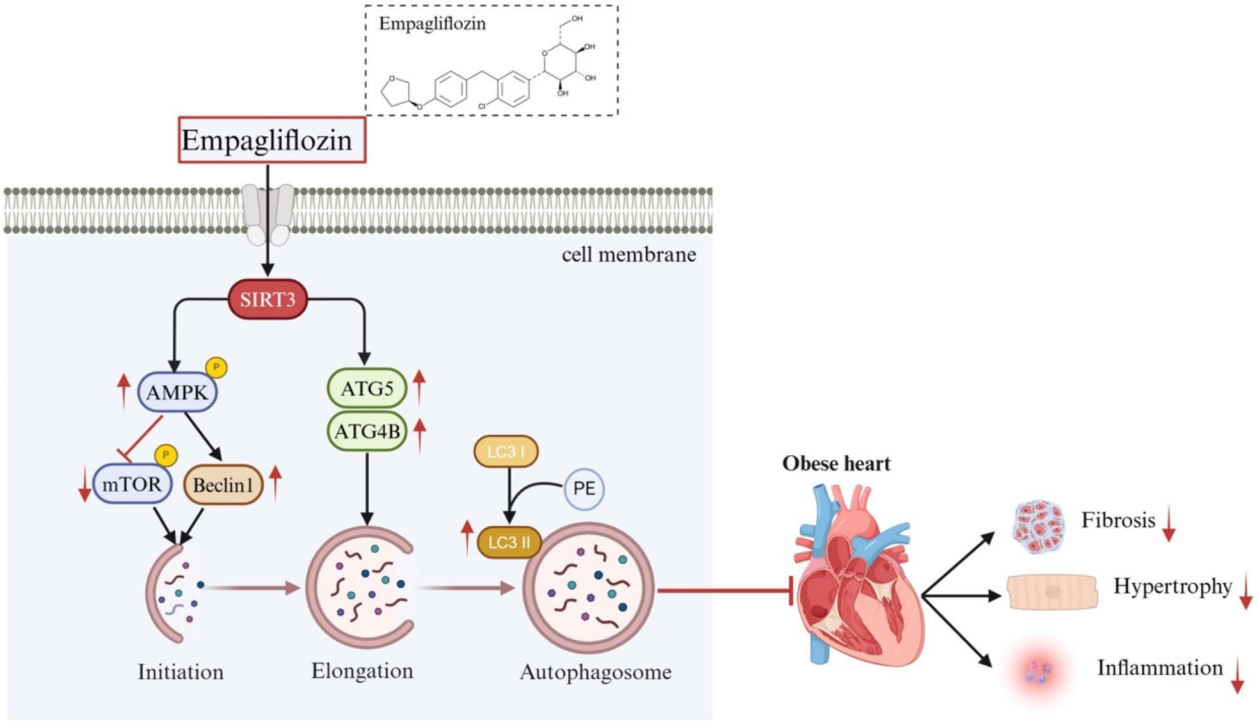

Fig. 7 EMPA upregulates SIRT3 to promote the formation and elongation of autophagosomes, thereby activating cardiac autophagy and inhibiting obesity-induced cardiac dysfunction

been confirmed that pathological cardiac hypertrophy is linked to dysfunction of the signaling pathways governing cardiomyocyte autophagy [8]. Therefore, preserving cardiac autophagic flux is important for maintaining cardiac function in the individuals with obesity. The present study revealed that EMPA intervention increased autophagy levels in the cardiac tissue of obese mice. To confirm that EMPA exerts cardioprotective effects by activating autophagy in cardiomyocytes, H9c2 cells were treated with the autophagy inhibitor 3-MA. These results demonstrated that after autophagy was inhibited, EMPA could no longer mitigate fibrosis, cellular hypertrophy, or elevated inflammation in cardiomyocytes. These findings suggest that autophagy is decreased in the hearts of obese mice and that EMPA can reverse this downregulation by increasing the number of various steps of autophagosome formation.

AMPK is the central regulator of energy metabolism and is considered an imperative therapeutic target for obesity, type II diabetes, and cancer [36]. The laboratory previously reported that EMPA activated the sestrin2-mediated AMPK/mTOR/p70S6K signaling pathway to attenuate cardiac hypertrophy by inhibiting myocardial proliferation in HFD-fed mice [32]. AMPK also controls the initiation of chaperone-mediated autophagy and further promotes the phagocytosis of damaged cardiomyocytes against hypoxia, ischemia, and oxidative stress [37]. In this study, HFD-induced obesity led to the inhibition of phosphorylated AMPK and the activation of mTOR, whereas EMPA reversed this cardiac response to initiate autophagy. Beclin1 acts as an overall scaffold for the class III PI3K complex involved in the initiation phase of autophagosome formation. Furthermore, EMPA induced the upregulation of Beclin1 in the hearts of obese mice, suggesting that EMPA also regulates the initiation of autophagy involving the Beclin1 pathway. In addition, studies have shown that AMPK phosphorylates Beclin1 at Thr388, which is an autophagy-specific domain, to induce autophagy [38]. These findings also suggest that EMPA activates the AMPK/mTOR pathway and further promotes the Beclin1-mediated autophagic pathway.

The ATG conjugation system and the processing of LC3 are responsible for the enlongation and maturation of autophagosomes. Notably, ATG4B is a key molecule in the elongation of autophagosomes, and it promotes the formation and breakdown of precursor LC3 and lipidated LC3 [39]. ATG5 forms a constitutive complex with ATG12 and further binds to Atg16L, which binds to the outer membrane of autophagosomes [40]. This complex promotes the stretching and expansion of the autophagosome [41], as well as the recruitment of LC3

I to the autophagosome [42]. The present study revealed that EMPA promoted the elongation of autophagosome membranes, LC3 I recruitment, and the formation of the autophagy marker LC3 II by increasing the expression of ATG4B, ATG5, and LC3 II. Therefore, EMPA is required to promote multiple steps of autophagy in obesity-induced cardiac structural and functional injury. However, knocking down SIRT3 in H9c2 cells did not restore ATG expression after EMPA intervention. These findings further suggest that EMPA promotes autophagy by increasing SIRT3 levels in obese cardiomyocytes.

Strengths and limitations of the study

The amelioration of autophagy is a critical factor in alleviating myocardial hypertrophy, fibrosis, and the inflammatory response. The current study provides a comprehensive understanding of the cardiac benefits of the SGLT2 inhibitor EMPA in the context of obesity via the promotion of SIRT3-mediated autophagosome formation. EMPA intervention activated SIRT3 in obese hearts, further initiating autophagy through AMPK phosphorylation and Beclin1 expression and encouraging ATG4B/ATG5-mediated autophagosome elongation. These findings highlight the intracellular mechanism of SGLT2 inhibitors in controlling the interplay between energy sensors and autophagy to improve obesity-induced cardiac dysfunction.

However, the impacts of EMPA were evaluated predominantly in wild-type mice in this research. Further testing of SIRT3-specific knockout mice could provide valuable insights into the biological functions of EMPA with respect to ORCD. Although the data from this study support that EMPA can improve obesity-induced myocardial hypertrophy, fibrosis, and the inflammatory response by promoting SIRT3-mediated autophagy, the specific combination and regulation of SIRT3 and EMPA still need further analysis.

Conclusions

Together, the results of the present study confirmed that EMPA has the ability to reduce ORCD efficiently through the SIRT3-mediated autophagy pathway. EMPA activated SIRT3-induced autophagy initiation via AMPK/Beclin1 and autophagosome membrane elongation via ATG4B/ATG5, which ultimately activated LC3II to induce the formation of myocardial autophagosomes. Clinical studies have revealed that autophagy is a useful marker for detecting left ventricular reverse remodeling during dilated cardiomyopathy, suggesting that autophagy is important for improving cardiac pathological remodeling. The key features of cardiac pathological remodeling are ventricular hypertrophy, inflammation, and fibrosis, which can be reversed by EMPA treatment during obesity. EMPA is an innovative option for reducing obesity-induced cardiac pathological remodeling, and the present findings suggest a novel mechanism by which EMPA regulates multiple aspects of autophagosome formation by enhancing SIRT3-mediated signaling pathways.

Abbreviations

ACC	Acetyl CoA carboxylase
AMPK	AMP-activated protein kinase
ATG4B	Autophagy-related 4B cysteine peptidase
ATG5	Autophagy-related 5
BNP	Brain Natriuretic Peptide
E/A	Early/late ventricular filling velocity
EF	Ejection Fraction
EMPA	Empagliflozin
FFA	Free Fatty Acids
FS	Fractional Shortening
GSK3β	Glycogen Synthase Kinase 3 beta
HFD	High-Fat Diet
IL-1β	Interleukin-1β
IL-18	Interleukin-18
ITT	Insulin tolerance test
mTOR	Mammalian Target Of Rapamycin
NLRP3	NLR family pyrin domain containing 3
OGTT	Oral Glucose Tolerance Test
ORCD	Obesity-Related Cardiac Dysfunction
PI3K	Phosphoinositide 3-Kinases
PINK1	PTEN-Induced Kinase 1
ROS	Reactive Oxygen Species
p70S6K	Ribosomal protein S6 Kinase, 70 kDa
α-SMA	α-Smooth Muscle Actin
SGLT2	Sodium-Glucose Cotransporter 2
SIRT3	Sirtuin 3
TG	Triglycerides
TGFβ	Transforming Growth Factor-β
TNF-α	Tumor Necrosis Factor-α
ULK1	Unc-51-Like Kinase 1
WGA	Wheat Germ Agglutinin

Supplementary Information

The online version contains supplementary material available at https://doi.org/10.1186/s12944-024-02293-9.

Supplementary Material 1

Supplementary Material 2

Acknowledgements

Not applicable.

Author contributions

LYH and YTT collected the data, conducted the analysis, and drafted the manuscript. ZJW and SXD designed the entire study and revised the manuscript. THZ and SHW participated in the data collection and analysis. KCX, HF and HNN examined the data and helped perform the analysis. The final manuscript has been read and approved by all authors.

Funding

This work was supported by the National Natural Science Foundation of China (82170865 and 82370856), Shandong Province Medical and Health Science and Technology Development Project (202203060917 and 202203060805), PhD Scientific Research Foundation (2022BSQD01) and Taishan Scholars Project of Shandong Province (tsqn202211365).

Data availability

No datasets were generated or analysed during the current study.

Declarations

Ethical approval
The animal study was approved by the Animal Ethics Committee of Shandong Second Medical University.

Competing interests
The authors declare no competing interests.

Author details
[1]Department of Endocrinology and Metabolism, Clinical Research Center, Shandong Provincial Key Medical and Health Discipline of Endocrinology, Affiliated Hospital of Shandong Second Medical University, Weifang 261031, China
[2]Department of Pathology, Affiliated Hospital of Shandong Second Medical University, Weifang 261031, China

Received: 22 May 2024 / Accepted: 11 September 2024
Published online: 27 September 2024

References
1. Kruszewska J, Cudnoch-Jedrzejewska A, Czarzasta K. Remodeling and fibrosis of the cardiac muscle in the course of obesity-pathogenesis and involvement of the extracellular matrix. Int J Mol Sci. 2022;23(8):4195.
2. Koliaki C, Liatis S, Kokkinos A. Obesity and cardiovascular disease: revisiting an old relationship. Metabolism. 2019;92:98–107.
3. Wang T, Cao Y, Zheng Q, Tu J, Zhou W, He J, et al. SENP1-Sirt3 signaling controls mitochondrial protein acetylation and metabolism. Mol Cell. 2019;75(4):823–e345.
4. Levine B, Kroemer G. Biological functions of autophagy genes: a disease perspective. Cell. 2019;176(1–2):11–42.
5. Kaludercic N, Maiuri MC, Kaushik S, Fernández ÁF, de Bruijn J, Castoldi F, et al. Comprehensive autophagy evaluation in cardiac disease models. Cardiovasc Res. 2020;116(3):483–504.
6. Rabinovich-Nikitin I, Rasouli M, Reitz CJ, Posen I, Margulets V, Dhingra R, et al. Mitochondrial autophagy and cell survival is regulated by the circadian clock gene in cardiac myocytes during ischemic stress. Autophagy. 2021;17(11):3794–812.
7. Shirakabe A, Zhai P, Ikeda Y, Saito T, Maejima Y, Hsu CP, et al. Drp1-dependent mitochondrial autophagy plays a protective role against pressure overload-induced mitochondrial dysfunction and heart failure. Circulation. 2016;133(13):1249–63.
8. Castañeda D, Gabani M, Choi SK, Nguyen QM, Chen C, Mapara A, et al. Targeting autophagy in obesity-associated heart disease. Obes (Silver Spring). 2019;27(7):1050–8.
9. Ren J, Wu NN, Wang S, Sowers JR, Zhang Y. Obesity cardiomyopathy: evidence, mechanisms, and therapeutic implications. Physiol Rev. 2021;101(4):1745–807.
10. Tong M, Mukai R, Mareedu S, Zhai P, Oka SI, Huang CY, et al. Distinct roles of DRP1 in conventional and alternative mitophagy in obesity cardiomyopathy. Circ Res. 2023;133(1):6–21.
11. Zhang T, Liu J, Tong Q, Lin L. SIRT3 acts as a positive Autophagy Regulator to promote lipid mobilization in Adipocytes via activating AMPK. Int J Mol Sci. 2020;21(2):372.
12. Wang S, Zhao Z, Fan Y, Zhang M, Feng X, Lin J, et al. Mst1 inhibits Sirt3 expression and contributes to diabetic cardiomyopathy through inhibiting parkin-dependent mitophagy. Biochim Biophys Acta Mol Basis Dis. 2019;1865(7):1905–14.
13. Thomas MC, Cherney D. The actions of SGLT2 inhibitors on metabolism, renal function and blood pressure. Diabetologia. 2018;61(10):2098–107.
14. Li HL, Lip G, Feng Q, Fei Y, Tse YK, Wu MZ, et al. Sodium-glucose cotransporter 2 inhibitors (SGLT2i) and cardiac arrhythmias: a systematic review and meta-analysis. Cardiovasc Diabetol. 2021;20(1):100.
15. Madonna R, Moscato S, Cufaro MC, Pieragostino D, Mattii L, Del Boccio P, et al. Empagliflozin inhibits excessive autophagy through the AMPK/GSK3β signalling pathway in diabetic cardiomyopathy. Cardiovasc Res. 2023;119(5):1175–89.
16. Hsieh PL, Chu PM, Cheng HC, Huang YT, Chou WC, Tsai KL, Chan SH. Dapagliflozin mitigates doxorubicin-caused myocardium damage by regulating AKT-mediated oxidative stress, Cardiac Remodeling, and inflammation. Int J Mol Sci. 2022;23(17):10146.
17. Hariharan R, Odjidja EN, Scott D, Shivappa N, Hébert JR, Hodge A, et al. The dietary inflammatory index, obesity, type 2 diabetes, and cardiovascular risk factors and diseases. Obes Rev. 2022;23(1):e13349.
18. Sun Z, Fang C, Xu S, Wang B, Li D, Liu X, et al. SIRT3 attenuates doxorubicin-induced cardiotoxicity by inhibiting NLRP3 inflammasome via autophagy. Biochem Pharmacol. 2023;207:115354.
19. Fan X, He Y, Wu G, Chen H, Cheng X, Zhan Y, et al. Sirt3 activates autophagy to prevent DOX-induced senescence by inactivating PI3K/AKT/mTOR pathway in A549 cells. Biochim Biophys Acta Mol Cell Res. 2023;1870(2):119411.
20. Ding W, Feng H, Li WJ, Liao HH, Tang QZ. Research progress on the interaction between autophagy and energy homeostasis in cardiac remodeling. Front Pharmacol. 2020;11:587438.
21. Yang H, Shen H, Li J, Guo LW. SIGMAR1/Sigma-1 receptor ablation impairs autophagosome clearance. Autophagy. 2019;15(9):1539–57.
22. Han D, Jiang L, Gu X, Huang S, Pang J, Wu Y, et al. SIRT3 deficiency is resistant to autophagy-dependent ferroptosis by inhibiting the AMPK/mTOR pathway and promoting GPX4 levels. J Cell Physiol. 2020;235(11):8839–51.
23. Hill SM, Wrobel L, Ashkenazi A, Fernandez-Estevez M, Tan K, Bürli RW, et al. VCP/p97 regulates beclin-1-dependent autophagy initiation. Nat Chem Biol. 2021;17(4):448–55.
24. Sheng Y, Song Y, Li Z, Wang Y, Lin H, Cheng H, et al. RAB37 interacts directly with ATG5 and promotes autophagosome formation via regulating ATG5-12-16 complex assembly. Cell Death Differ. 2018;25(5):918–34.
25. Packer M. Critical reanalysis of the mechanisms underlying the Cardiorenal benefits of SGLT2 inhibitors and reaffirmation of the nutrient Deprivation Signaling/Autophagy hypothesis. Circulation. 2022;146(18):1383–405.
26. Lu Q, Liu J, Li X, Sun X, Zhang J, Ren D, et al. Empagliflozin attenuates ischemia and reperfusion injury through the LKB1/AMPK signaling pathway. Mol Cell Endocrinol. 2020;501:110642.
27. Lin K, Yang N, Luo W, Qian JF, Zhu WW, Ye SJ, et al. Direct cardio-protection of Dapagliflozin against obesity-related cardiomyopathy via NHE1/MAPK signaling. Acta Pharmacol Sin. 2022;43(10):2624–35.
28. Furman D, Campisi J, Verdin E, Carrera-Bastos P, Targ S, Franceschi C, et al. Chronic inflammation in the etiology of disease across the life span. Nat Med. 2019;25(12):1822–32.
29. Neeland IJ, Poirier P, Després JP. Cardiovascular and metabolic heterogeneity of obesity: clinical challenges and implications for management. Circulation. 2018;137(13):1391–406.
30. Zinman B, Wanner C, Lachin JM, Fitchett D, Bluhmki E, Hantel S, et al. Empagliflozin, cardiovascular outcomes, and mortality in type 2 diabetes. N Engl J Med. 2015;373(22):2117–28.
31. Fitchett DH. Empagliflozin and cardio-renal outcomes in patients with type 2 diabetes and cardiovascular disease - implications for clinical practice. Eur Endocrinol. 2018;14(2):40–9.
32. Sun X, Han F, Lu Q, Li X, Ren D, Zhang J, et al. Empagliflozin ameliorates obesity-related cardiac dysfunction by regulating sestrin2-mediated AMPK-mTOR signaling and redox homeostasis in high-fat diet-induced obese mice. Diabetes. 2020;69(6):1292–305.
33. Nasiri-Ansari N, Nikolopoulou C, Papoutsi K, Kyrou I, Mantzoros CS, Kyriakopoulos G, et al. Empagliflozin attenuates non-alcoholic fatty liver disease (NAFLD) in high fat diet fed ApoE$^{-/-}$ mice by activating autophagy and reducing ER stress and apoptosis. Int J Mol Sci. 2021;22(2):818.
34. Zhang Q, Siyuan Z, Xing C, Ruxiu L. SIRT3 regulates mitochondrial function: a promising star target for cardiovascular disease therapy. Biomed Pharmacother. 2024;170:116004.
35. Kanamori H, Naruse G, Yoshida A, Minatoguchi S, Watanabe T, Kawaguchi T, et al. Metformin enhances autophagy and provides cardioprotection in δ-sarcoglycan deficiency-induced dilated cardiomyopathy. Circ Heart Fail. 2019;12(4):e005418.
36. Jeon SM. Regulation and function of AMPK in physiology and diseases. Exp Mol Med. 2016;48(7):e245.
37. Song X, Zhu S, Chen P, Hou W, Wen Q, Liu J, et al. AMPK-mediated BECN1 phosphorylation promotes ferroptosis by directly blocking dystem X_c^- activity. Curr Biol. 2018;28(15):2388–e995.
38. Zhang D, Wang W, Sun X, Xu D, Wang C, Zhang Q, et al. AMPK regulates autophagy by phosphorylating BECN1 at threonine 388. Autophagy. 2016;12(9):1447–59.
39. Sun L, Xiong H, Chen L, Dai X, Yan X, Wu Y, et al. Deacetylation of ATG4B promotes autophagy initiation under starvation. Sci Adv. 2022;8(31):eabo0412.

40. Lin TY, Chan HH, Chen SH, Sarvagalla S, Chen PS, Coumar MS, et al. BIRC5/Survivin is a novel ATG12-ATG5 conjugate interactor and an autophagy-induced DNA damage suppressor in human cancer and mouse embryonic fibroblast cells. Autophagy. 2020;16(7):1296–313.
41. Qiang L, Yang S, Cui YH, He YY. Keratinocyte autophagy enables the activation of keratinocytes and fibroblastsand facilitates wound healing. Autophagy. 2021;17(9):2128–43.
42. Xiang H, Liu R, Zhang X, An R, Zhou M, Tan C, et al. Discovery of small-molecule autophagy inhibitors by disrupting the protein-protein interactions involving autophagy-related 5. J Med Chem. 2023;66(4):2457–76.

Publisher's note